

Spin depolarization in the transport of holes across GaMnAs/GaAlAs/p-GaAs

L.Brey,¹ J.Fernández-Rossier,² and C.Tejedor³

¹*Instituto de Ciencia de Materiales de Madrid (CSIC), Cantoblanco, 28049, Madrid, Spain.*

²*Departamento de Física Aplicada, Universidad de Alicante, 03690 Alicante, Spain.*

³*Departamento de Física Teórica de la Materia Condensada,
Universidad Autónoma de Madrid, 28049 Madrid, Spain.*

(Dated: May 23, 2019)

We study the spin polarization of tunneling holes injected from ferromagnetic GaMnAs into a p-doped semiconductor through a tunneling barrier. We obtain an upper limit to the spin injection rate. We find that spin-orbit interaction interaction in the barrier and in the drain limits severely spin injection. Spin depolarization is stronger when the magnetization is parallel to the current than when is perpendicular to it.

PACS numbers: 75.50.Pp, 75.25.DcLp

Achieving the injection of spin polarized current from a ferromagnetic material into a semiconductor is one of the challenges in spintronics^{1,2}. However, the conductivity mismatch between ferromagnetic metals and semiconductors prevents simple strategies of spin injection in the diffusive regime^{3,4}. At least two kind of proposals have been suggested in order to circumvent this obstacle. First, the use of a tunnel barrier between the ferromagnetic source and the semiconductor⁵. Second the use of diluted magnetic semiconductors (DMS) as a source^{6,7}.

Ferromagnetic diluted magnetic semiconductors materials like GaMnAs have raised enormous interest both because of their fundamental interest and their potential in spintronics proposals. One of the appealing features of of GaMnAs and other DMS is that they can be integrated easily with other III-V based heterostructures combining the magnetic and electronic functionalities. In this direction heterostructures based in GaMnAs have been grown that feature strong tunneling magneto resistance effects^{8,9}. On the other side, the Curie Temperature is still below room temperature although improvement in post growth annealing techniques^{10,11} in GaMnAs DMS shows the ability to obtain critical temperatures larger than 150K.

In GaMnAs, Mn act as an acceptor that supplies holes responsible for the long range ferromagnetic interaction between the Mn spins^{12,13,14}. Crucial in the understanding of the ferromagnetic phase of the material is the fact that the spin-orbit interaction for the valence band holes is very strong ($\Delta \sim 340$ meV). This large spin-orbit coupling has several effects on the properties of magnetic GaMnAs: *i)* There is a large correlation between T_c and strength of the spin-orbit interaction¹² *ii)* Spin-orbit, combined with strain effects due to the substrate-DMS lattice mismatch, determines the easy-axis for the magnetization¹⁵. *iii)* Spin-orbit is also responsible for the anisotropic magneto resistance in bulk GaMnAs^{16,17}.

In this work we address the effect of spin-orbit coupling on the injection of a spin polarized hole current from a DMS into a p-doped paramagnetic semiconductor, via

an epitaxially grown tunnel junction, *i.e.*, in the coherent regime. In particular we want to analyze how the spin polarization is degraded, and how the spin current polarization depends on the angle formed by the electrical current and the magnetization. These two questions are relevant for the possible use of GaMnAs as a source of spin polarized current. The system of interest consists of a ferromagnetic semiconductor and a non magnetic semiconductor separated by a tunnel barrier. In particular, the left electrode is GaMnAs, the right electrode is p-doped GaAs and the barrier is GaAlAs. We consider that transport takes place by tunneling through a GaAlAs barrier of width d . In this configuration spin-orbit coupling is the same along the whole heterostructure. We also analyze the effect produced by the quenching of the spin-orbit coupling only at the drain or both at the drain and the barrier. We anticipate the main conclusions of this work:

1) Spin-orbit coupling, both at the drain and at the barrier, significantly reduces the spin polarization of carriers injected into the non magnetic electrode.

2) Spin injection depends significantly on the angle between the current flow and the magnetization of the source electrode. When the magnetization at the source is parallel to the electrical current, the depolarization effect is stronger than for the case of source magnetization perpendicular to the current.

Theoretical approach: The system considered is formed by three well defined regions along the growth direction (z). The *left region* (L) is the source for the spin polarized current and is formed by GaMnAs. The *barrier region* (B) is formed by GaAlAs while the *right region* (R) is a paramagnetic p-doped semiconductor, for example Be-doped GaAs. The valence bands of this system is described in a $\mathbf{k} \cdot \mathbf{p}$ framework by means of a Hamiltonian

having three parts:

$$\begin{aligned} H^L &= H_{\mathbf{k} \cdot \mathbf{p}}^L + J_{pd} N_{Mn} S m \vec{\Omega} \cdot \vec{s} \\ H^B &= H_{\mathbf{k} \cdot \mathbf{p}}^B + \Delta V^{L-B} \\ H^R &= H_{\mathbf{k} \cdot \mathbf{p}}^R + \Delta V^{L-R}. \end{aligned} \quad (1)$$

$H_{\mathbf{k} \cdot \mathbf{p}}^L$, $H_{\mathbf{k} \cdot \mathbf{p}}^B$ and $H_{\mathbf{k} \cdot \mathbf{p}}^R$ are six band Kohn-Luttinger Hamiltonians for L, B and R, respectively^{12,13}. Ternary compounds GaMnAs and GaAlAs are described a virtual crystal approximation (VCA). We use the same Kohn-Luttinger parameters to describe the electronic properties of GaAs, GaMnAs and GaAlAs, i.e. $H_{\mathbf{k} \cdot \mathbf{p}}^R = H_{\mathbf{k} \cdot \mathbf{p}}^L = H_{\mathbf{k} \cdot \mathbf{p}}^B$.

In GaMnAs exchange interaction couples the spin of valence band holes with the spin of the Mn ions, which are randomly located in the cation sublattice. In the mean field and VCA¹², the disordered exchange interaction is replaced by a homogeneous effective Zeeman field. This approach accounts for a number of experimental observations. The second term of H^L describes the coupling of the holes to the effective field. There, J_{pd} is the exchange coupling, N_{Mn} the Mn ion density, S the spin of a Mn ion, m the spin polarization of the Mn spins, $\vec{\Omega}$ the orientation of the magnetization and \vec{s} the spin of the holes. In this theoretical framework, the ferromagnetic electrode is characterized by the density of Mn and the density of holes. For a given set of parameters in the model we obtain the spin polarization of both Mn and holes¹⁴.

The GaAlAs barrier and p-doped GaAs drain are described by means of $k \cdot p$ Hamiltonians with shifts ΔV^{L-B} and ΔV^{L-R} with respect to the top of the valence band of the ferromagnetic semiconductor. The precise value of the barrier height ΔV^{L-B} depends on the Al content in the barrier. We have verified that our results are not very sensitive to this parameter and we take $\Delta V^{L-B} = 300$ meV. The shift ΔV^{L-R} permits to have a different carrier density in the p-doped region with a common Fermi energy across the heterostructure. Our rigid-band model neglects band-bending effects across the interfaces¹⁸.

Charge and spin transport are studied in the scattering formalism^{19,20,21}. The quantum states of the electrodes are described by a band index n and a wave vector \mathbf{k} , in the framework of the six band $\mathbf{k} \cdot \mathbf{p}$ approximation. These states are linear combination of p -like orbitals with total angular momenta $J=3/2$ and $J=1/2$. In the presence of spin-orbit coupling, the spin is not a good quantum number so that the quantities conserved in the tunneling process are the energy, E , and the parallel component of the wave vector, k_{\parallel} ^{19,20}. An incoming plane-wave state from L, $|n, E, k_{\parallel}; L\rangle$, is transmitted to a plane wave $|n', E, k_{\parallel}; R\rangle$ at R with a transmission amplitude $t_{n,n'}^{k_{\parallel}}(E)$. As the group velocity in the left and right regions are in general different, the transmission probability from a state $|n, E, k_{\parallel}; L\rangle$ to a state $|n', E, k_{\parallel}; R\rangle$

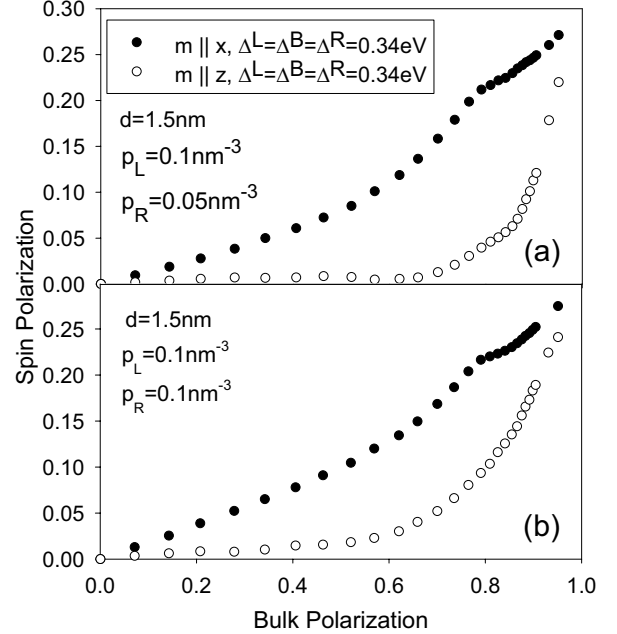


FIG. 1: Spin polarization η_{tr} as a function of the bulk polarization of GaMnAs along two different directions.

reads¹⁹

$$T_{n,n'}^{k_{\parallel}}(E) = |t_{n,n'}^{k_{\parallel}}(E)|^2 \frac{v_{n'}(E, k_{\parallel}; R)}{v_n(E, k_{\parallel}; L)}, \quad (2)$$

where $v_n(E, k_{\parallel}; L/R)$ is the group velocity, along the z -direction perpendicular to the interfaces, of the state $|n, E, k_{\parallel}; L/R\rangle$. In our calculation, only incoming and transmitted states with positive group velocity are considered. In this approach, the linear conductance of the heterostructure can be obtained as a sum over all transmission channels, $G = (e^2/h) \sum_{n,n',k_{\parallel}} T_{n,n'}^{k_{\parallel}}(E_F)$.

In the following we study the degradation of the spin polarization of carriers passing from the source (GaMnAs) to a paramagnetic drain. We define the spin polarization of the transmitted current,

$$\eta_{tr} = 2 \frac{\sum_{n,n',k_{\parallel}} T_{n,n'}^{k_{\parallel}}(E_F) \langle n', k_{\parallel}, E_F; R | s | n', k_{\parallel}, E_F; R \rangle}{\sum_{n,n',k_{\parallel}} T_{n,n'}^{k_{\parallel}}(E_F)} \quad (3)$$

where s is the component of the hole spin along $\vec{\Omega}$. We have verified that η_{tr} along other directions vanishes. This quantity describes the spin polarization of the coherently transmitted holes. Inelastic events which can result in further spin relaxation after tunneling are not included in our approach. Therefore, η_{tr} represents an upper limit to the spin injection which can be obtained in the experiment.

Results: In Fig. 1, we show the spin polarization of the transmitted current, η_{tr} , as a function of the bulk polarization of GaMnAs, η_0 . At this point it is convenient

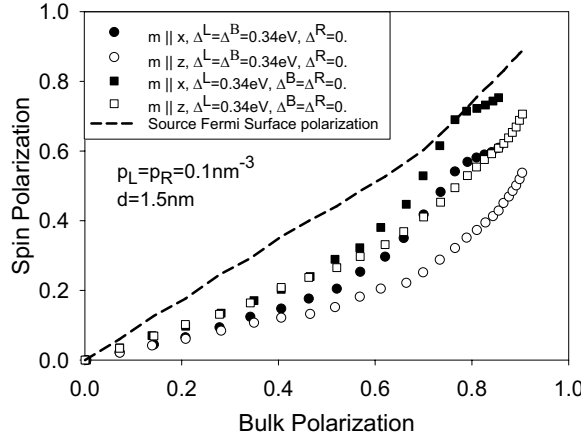


FIG. 2: Spin polarization η_{tr} as a function of the bulk polarization of GaMnAs along two different directions. Results are for zero spin-orbit coupling only at R (circles) or at R and B (squares). Dashed line shows the spin polarization at the Fermi level of GaMnAs.

to distinguish between the bulk polarization of GaMnAs, η_0 , and the polarization of the holes in the Fermi surface of this material, η_F ²². The carrier density at the ferromagnetic source is fixed, $p_L = 0.1 \text{ nm}^{-3}$, while two different values of p_R are considered. Two different magnetization orientation of the ferromagnetic electrode are studied, either parallel or perpendicular to the current flow, chosen along z . Results in Fig. 1, are obtained with the same spin-orbit coupling constant, $\Delta = 0.34 \text{ eV}$, in all the three regions. It is notorious that η_{tr} is significantly smaller than the bulk polarization of the injector. The depolarization is stronger when the carriers are polarized parallel to the current (z) (open circles) than when they are polarized along x , i.e. perpendicular to the current (black circles). This effect is larger in the case with lower density p_R of carriers in the p-GaAs. The feature appearing in η_{tr} for $\eta_0 \simeq 0.8$, for current perpendicular to the magnetization, coincides with the complete depopulation of a band of minority-spin carriers in GaMnAs.

The strong depolarization of coherently injected spins is produced by three mechanisms:

First: Reduction of the spin polarization at the Fermi surface. At small bias, only electrons at the Fermi level are injected. As it happens, the hole spin polarization at the Fermi energy η_F is smaller than the bulk spin polarization η_0 (dashed line of Fig. 2). The ratio η_F/η_0 is roughly 0.9 for $\eta_0 < 0.65$ and even larger as η_0 approaches to 1. Therefore, this effect is small in general.

Second: Spin-orbit coupling at the barrier and the drain. Fig. 2 shows η_{tr} when spin-orbit coupling is removed either in the p-doped GaAs region or both in the barrier and p-doped region. The spin injection rate is significantly higher than the case of Fig. 1, showing that spin-orbit interaction is detrimental for successful spin

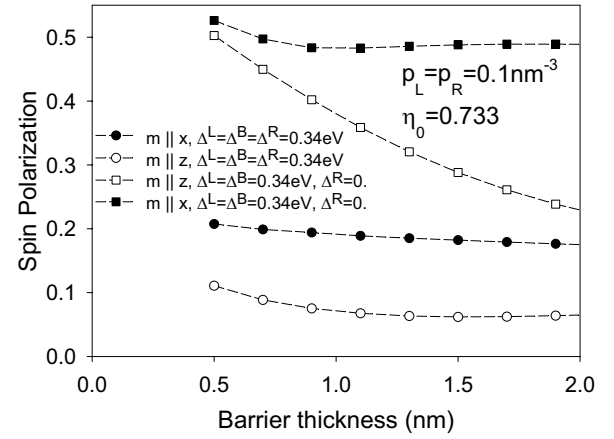


FIG. 3: Spin polarization η_{tr} as a function of the barrier width d for magnetization along two different directions.

injection. This is corroborated by the fact that polarizations are larger (lower depolarizations) when spin-orbit coupling is removed both at the barrier and the p-doped semiconductor. As in the case of Fig. 1, depolarization is stronger when carriers are polarized along the current direction. The directional dependence is also weaker indicating that in the case of Fig. 1 it comes from the the spin-orbit interaction of both electrodes and barrier.

Third: Spin mixing and spin filtering in the barrier. Even in the absence of spin-orbit interaction in the barrier, tunnel probability can be spin dependent. This is known as spin filtering and accounts for the difference between squares (spin-orbit only in the source) and dashed line in Fig. 2. In order to clarify the effect of the barrier in the depolarization, Fig. 3 shows η_{tr} as a function of the barrier width. The set of parameters is: 0.733 for the polarization of GaMnAs (slightly below the kink in Fig. 2), $p_L = p_R = 0.1 \text{ nm}^{-3}$. We give results for the two orientations of the polarization as in Figs. 1 and 2, and both with and without spin-orbit coupling at R. When carriers are polarized perpendicular to the current, there are not significant variations due to d . This indicates that, in this case, no important effects come from the barrier as it occurred in Fig. 2. On the contrary, when carriers are polarized along z and no spin-orbit coupling is included at R, η_{tr} increases rapidly with decreasing d . For this direction of the polarization, band mixing effects are important.

Finally, let us discuss the cause of the large difference observed for depolarizations along the two orientations x and z . For this purpose, we analyze what happens at the Fermi level at L in the range of parameters around the value of η_0 for which one of the bands becomes empty. Fig. 4 shows carrier velocities and spins for each band at the Fermi level of GaMnAs. As mentioned above, only

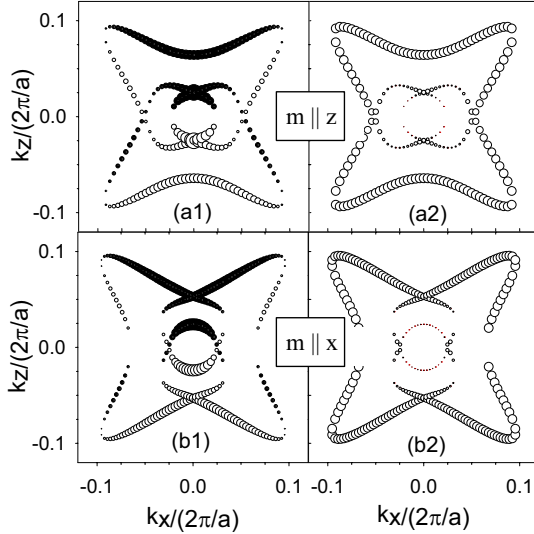


FIG. 4: Carrier velocities $v_n(E, k_{\parallel}; L)$ (left side) and expectation value of the spin component along the direction of the polarization (right side) in a contour at the Fermi level of GaMnAs. Black/white circles depict positive/negative velocities at the left and positive/negative spins at the right. The magnitude of velocities and spins is depicted by the size of the circles. Results correspond to $\eta_0=0.82$

states with positive velocities are taken into account to compute the conductance. States with small velocities give the dominant contribution because $v_n(E, k_{\parallel}; L)$ appears at the denominator of Eq. (2). Fig. 4 shows that these states carry a larger spin for polarization along x than for polarization along z . This makes the former the optimal direction for injecting spin as shown in all the results in Figs. 1-3.

In summary, spin-orbit coupling has a strong influence on the spin injection of holes from ferromagnetic GaMnAs into p-doped GaAs via a tunneling barrier. First of all, spin-orbit interaction reduces severely the efficiency of spin injection. Therefore, prospects of hole spin injections seem better for materials with small spin-orbit like Si or GaN. Secondly, the spin injection rate depends on the angle between current flow and magnetization. In particular, spin injection is significantly larger for samples magnetized parallel to the interfaces of the heterostructure.

We are indebted to G. Platero for the critical reading of the manuscript. Work supported in part by MCYT of Spain under contract Numbers MAT2002-04429-C03-01, MAT2002-00139, MAT2003-08109-C02-01, Fundación Ramón Areces, Ramon y Cajal program and UE within the Research Training Network COLLECT.

¹ Y.Ohno, in *Semiconductor spintronics and quantum computation*, edited by D.D.Awschalom, D.Loss, and N.Samarth (Springer-Verlag, New York, 2002).

² S. Datta and B. Das, *Appl. Phys. Lett.* **56**, 665 (1990).

³ G. Schmidt, D.Ferrand, L.W.Molenkamp, A.R.Filip, and B. van Wees, *Phys. Rev. B* **62**, R4790 (2000).

⁴ C.-M. Hu and T. Matsuyama, *Phys. Rev. Lett.* **87**, 066803 (2001).

⁵ E. I. Rashba, *Phys. Rev. B* **62**, R16267 (2000).

⁶ R.Fiederlin, G.Reuscher, W. Ossau, G.Schmidt, A.Wang, and L.W.Molenkamp, *Nature* **402**, 787 (1999).

⁷ Y. Ohno, D. K. Young, B. Beschoten, F. Matsukura, H. Ohno, and D. D. Awschalom, *Nature* **402**, 790 (1999).

⁸ M.Tanaka and Y.Higo, *Phys. Rev. Lett.* **87**, 026602 (2001).

⁹ R.Mattana, J.-M.George, H.Jaffres, F. V. Dau, A.Fert, B.Lepine, A.Guivarc'h, and G.Jezequel, *Phys. Rev. Lett.* **90**, 166601 (2003).

¹⁰ S. J. Potashnik, K. C. Ku, S. H. Chun, J. J. Berry, N. Samarth, and P. Schiffer, *Appl. Phys. Lett.* **79**, 1495 (2001).

¹¹ K. Edmonds, K. Wang, R. Campion, A. Neumann, N. Farley, B. Gallagher, and C. Foxon, *Appl. Phys. Lett.* **81**, 4991 (2002).

¹² T. Dietl, H. Ohno, F. Matsukura, J. Cibert, and D. Ferrand, *Science* **287**, 1019 (2000).

¹³ M. Abolfath, T. Jungwirth, J. Brum, and A. MacDonald, *Phys. Rev. B* **63**, 054418 (2001).

¹⁴ L.Brey and G.Gómez-Santos, *Phys. Rev. B* **68**, 115206 (2003).

¹⁵ H. Ohno, *Science* **281**, 951 (1998).

¹⁶ T. Jungwirth, M. Abolfath, J. Sinova, J. Kucera, and A. MacDonald, *Appl. Phys. Lett.* **81**, 4029 (2002).

¹⁷ D. D. A. H. X. Tang, R. K. Kawakami and M. L. Roukes, *Phys. Rev. Lett.* **90**, 107201 (2003).

¹⁸ J. Fernandez-Rossier and L. J. Sham, *Phys. Rev. B* **64**, 235323 (2001).

¹⁹ R.Wessel and M.Altarelli, *Phys. Rev. B* **39**, 12802 (1989).

²⁰ Y.X.Liu, D.Z.-Y.Ting, and T.C.McGill, *Phys. Rev. B* **54**, 5675 (1996).

²¹ A. G. Petukhov, A. N. Chantis, and D. O. Demchenko, *Phys. Rev. Lett.* **89**, 107205 (2002).

²² I. I. Mazin, *Phys. Rev. Lett.* **83**, 1427 (1999).